JOURNAL OF MATERIALS SCIENCE 28 (1993) 5880–5886

Failure mechanisms in mission-cycled carbon/carbon composites under flexural load at room and elevated temperatures

H. MAHFUZ, P. S. DAS, S. JEELANI
Materials Research Laboratory, Tuskegee University, Tuskegee, AL, USA
D. M. BAKER, S. A. JOHNSON
General Dynamics, Fort Worth, TX, USA

The response of quasi-isotropic laminates of SiC coated carbon/carbon (C/C) composites under flexural load was studied. Mission-cycled as well as virgin specimens were tested to compare the thermal- and pressure-cycling effects. Variation of flexural strength and stiffness with temperature was investigated to study the load–deflection behaviour and the thermal stability of C/C composites up to 1371 °C. Increase in flexural strength and stiffness were observed with the rise in temperature. A distinct shift in failure modes from compressive to tensile was found with the mission-cycled specimens with the increase in test temperatures, while the failure mode for virgin material was found always on the tensile side. Change in the load–deflection behaviour was examined and increase in non-linearity of the stress–strain behaviour with the mission cycling was observed. Although the number of test specimens was few, Weibull characterization on the flexure data was performed to study the variation of Weibull modulii and the characteristic lives. Failed, as well as untested, specimens were C-scanned to identify the location and the extent of the damaged zone. Post-failure analyses through optical microscopy and scanning electron microscopy were performed to study the damage growth and failure mechanisms. Degradation and separation of the porous matrix structure, localized damage of the reinforcing fibres in the transverse direction, complete fibre bundle failure in the mission-cycled specimens, and delamination near the loading zone were observed.

1. Introduction

Research on carbon/carbon C/C composites goes back almost two decades, but only after its successful use as thermal protection system in the wing leading edge and nose cap of the space shuttle, did it come into prominence. These earliest forms of C/C are well characterized and, in fact, were the first to show that C/C composites remain viable structural materials at temperatures up to 2204 °C (4000 °F) [1–3], including the unusual attribute of increasing strength with increasing temperature up to 2204 °C [4]. This unique behaviour combined with resistance to catastrophic failure by fibre toughening, good thermal shock resistance and densities below 2 $g\,cm^{-3}$ makes C/C composites the primary candidate for application where operating temperature exceeds 1093 °C (2000 °F). This high-temperature capability and its low atomic number gives C/C much superior resistance to both laser and nuclear weapon X-ray threats [5].

Although C/C composites possess attractive mechanical and physical properties at high temperature, their application as structural materials is currently limited by the susceptibility of carbonaceous materials to oxidation and gasification at elevated temperature. In the absence of a protective coating to inhibit oxidation reactions, carbon fibres can begin to degrade considerably in air at temperatures as low as 400 °C [6]. Therefore, the use of graphitic C/C composites in applications such as rocket nozzles, gas turbine blades, automobile and aeronautical disc brakes necessitates the development of oxidation-resistant composites which are capable of resisting oxidation at temperatures in excess of 1500 °C [7]. Much effort is therefore needed to develop techniques for protecting carbon fibre-reinforced materials against oxidation at high temperatures. A potential problem concerning the oxidation protection is the thermal expansion mismatch between the coating and the substrate. Damage initiation in C/C composites during flexural loading has been reported by some researchers [8]. The analysis has been performed at room temperature with uncoated specimens. Two fundamental aspects, namely, the effects of coating and temperature, have not been studied, which we believe will have considerable influence in the damage mechanisms of C/C. A thorough understanding of the surface chemistry

0022–2461

and the oxidation kinetics related to the substrate is therefore required. The matrix in C/C composites is produced either by chemical vapour deposition (CVD) or by impregnation with a carbonaceous liquid pitch or resin followed by carbonization and graphitization. Both methods produce porosity during the carbonization process [9]. In addition, cracks are produced because of the thermal expansion mismatch between the fibre and the carbon matrix. Several infiltration cycles are usually employed, often using successively less viscous infiltrants to obtain materials with desired density. However, the problem of porosity and crack generation at the interface still exists to this day. Moreover, two-dimensional composites which are most generally used because of their cost and fabrication flexibility, have inherent anisotropy including poor mechanical properties in the interlaminar direction [10].

The response of composite materials to any applied load is dependent on the fibre, matrix and the fabrication process, and their performance has been observed to scatter to a large extent [11]. This is because of the fact that flaws are inherent in the composite material from the very fabrication process. From this point of view, the Weibull analysis on the performance of the material is an important area of investigation. It is also well known that a complex damage state is developed in the composite during mechanical loading [12]. To asses this damage, either during fabrication or loading, non-destructive evaluation (NDE) is a reliable technique [13]. In this paper the flexural response of SiC coated C/C composites (ACC-4) is presented at room and elevated temperatures. Virgin and mission-cycled specimens have been tested in three-point bending. The variation in flexural strength and stiffness were examined. The load–deflection behaviour of the material at various temperatures has been investigated, and the Weibull [14] analysis of the flexural data has been performed. Micrographs of various cross-sections were taken in the damaged zone using OM and SEM, and the failure mechanisms were discussed. Untested as well as fractured specimens have been C-scanned to identify the damaged zone and visualize the extent of the damage. Failure analyses on the basis of the NDE, micrographs and experimental data are presented.

2. Experimental procedure

2.1. Material and specimen preparation

The fabrication of the material began with satin woven cloth of 3k T-300 yarns which was converted into graphite and impregnated with a phenolic resin. This impregnated cloth was laid up in $[+45, 90, -45, 0]_s$ sequence to form the laminate, and was cured in an autoclave. After curing, the laminate was pyrolysed at high temperature to convert the resin to carbon. To improve the structure of the porous matrix the laminate was then carbon impregnated. This impregnation and pyrolysis was repeated four times to achieve the desired density of about 1.6 g cm^{-3}. A fibre volume fraction of 64% was maintained in the final uncoated specimens. The specimens were then pack cemented with SiC coating which was embedded with glass sealants. The coating thickness was maintained between 100 and 120 μm. To simulate the effects of temperature and pressure in a typical ground to orbital flight of a hypersonic vehicle, a number of specimens were test cycled through a pressure–temperature cycle as shown in Fig. 1. Test cycles were limited to 5 and 10, and these specimens were termed 5 or 10 "mission-cycled specimens". On the other hand, the specimens that were not mission-cycled were termed "virgin". All flexure tests were conducted on a three-point beam. The loading and the specimen dimensions are shown in Fig. 2.

2.2. Flexure test

The flexural strength and stiffness for virgin as well as mission-cycled specimens were determined at room temperature, 649 °C (1200 °F) and 1371 °C (2500 °F) in air by using a three-point bend test. All the flexural tests were carried out according to ASTM standard D-790. An Instron 8502 test machine with series-IX data acquisition system was used. For high-temperature tests, the three-point bend fixture was fabricated from cast SiC and the push rods were made of alumina. The outer and inner spans of the specimen are shown in Fig. 2. The crosshead speed for all tests was 0.05 in. min^{-1} (1.27 mm min^{-1}). The equations used for evaluating the flexural strength and stiffness were the typical three-point beam equations derived from the Euler–Bernoulli beam theory [15]. During the

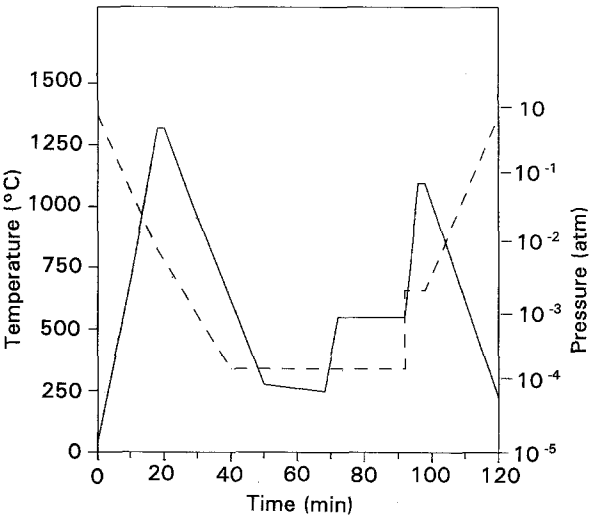

Figure 1 Pressure–temperature cycle for mission cycling. (- - -) Pressure, (——) temperature.

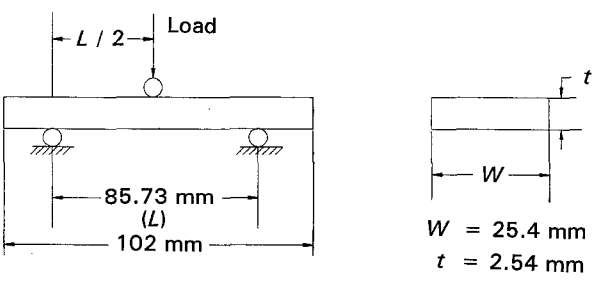

Figure 2 Specimen dimensions and loading.

high-temperature tests, the furnace was heated gradually at a rate of 10 °C min^{-1}. After reaching the test temperature, the isothermal condition was maintained for about half an hour during which the test was conducted and then the furnace was cooled down, again at 10 °C min^{-1}.

2.3. Optical microscopy and scanning electron microscopy

The failed specimens were cut into small samples using an Excel diamond cutter along the longitudinal and transverse directions. The fractured surfaces were then exposed to the optical microscope, using polarized light. For scanning electron micrographs, these samples were mounted on an aluminium stub and coated with gold to prevent charging during the subsequent examination by SEM.

2.4. Non-destructive evaluation

The non-destructive evaluation of the fractured as well as untested specimens was performed in a Test Tech ultrasonic scanning machine equipped with DAS-100 data acquisition system. Sound in the 10 MHz frequency range was produced by pulsing a lithium sulphite transducer which also functioned as the receiver element. The resulting waveform was digitized to 8 bits and processed by the microcomputer. The microcomputer also controlled the movement of the x–y scanner. The imaging of the data obtained through the ultrasonic scanning for various specimens was stored and eventually plotted via a TEK 4696 colour printer with an intensity of 120 × 120 DPI.

3. Results and discussion

Flexural tests were conducted at room temperature (RT), 649 °C (1200 °F) and 1371 °C (2500 °F) to determine the flexural strength as well as stiffness of virgin, 5 and 10 mission-cycled specimens. The variation of flexural strength with temperatures for three types of specimens is shown in Fig. 3. Considerable increase in strength from room temperature to 1371 °C is observed with all categories of materials. Visual observations indicated that all failures were on the tensile side for virgin specimens. For mission-cycled specimens, failure was on the compression side at RT, and on the tensile side at elevated temperatures. Both at RT and at elevated temperatures, a crack initiated in the virgin specimens from the outer surface of the tensile face due to its coating failure. The crack could not penetrate through the fibre bundle because of the weak interfacial bonding between the fibre and the matrix. Because of this weak interface, load is not transferred efficiently from the matrix to the fibres; thus properties of the reinforcement are not utilized, which gives low matrix fracture stress and low ultimate strength at RT [16]. At high temperature, the matrix expands, giving the load-carrying fibres more support, and simultaneously helps increase the strength. However, the case is completely different for mission-cycled materials. Interfacial bonding becomes stronger and stronger

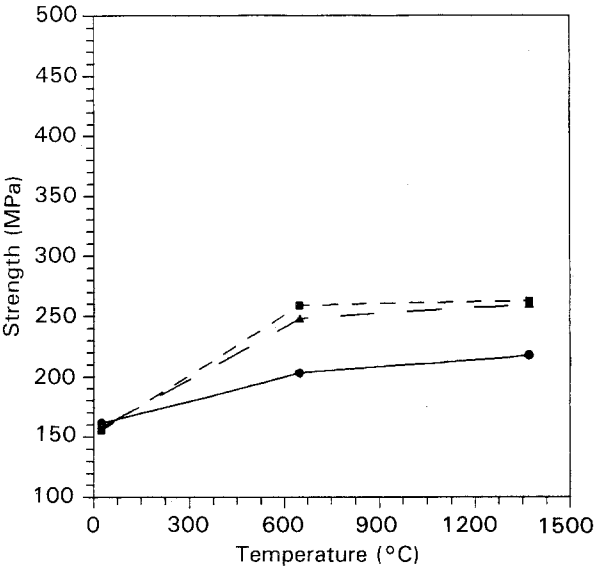

Figure 3 Flexural strength variation with temperatures. (●) Virgin, (■) 5, and (▲) 10 mission specimens.

because of the mission cycling, which causes both the fibres and matrix to be responsible for carrying the load. At RT with the mission-cycled specimens, it was observed that the crack also initiated on the tensile side similar to what was found with the virgin specimens. But the final failure of the specimens was noticed on the compression side. At elevated temperature, expansion of the matrix increases its compressive load-carrying capability and simultaneously allows the initial crack on the tensile side to propagate along the fibre bundle through the matrix region. This helps the fibre bundle to carry the load for a longer period of time before the crack can penetrate through it, thus increasing the strength. At higher temperatures the failure of the specimen is clearly due to the tensile failure of the fibre. This gives higher strength at elevated temperatures. A similar phenomenon in the case of three-dimensional C/C has been reported by Robinson [17]. The 5 and 10 mission-cycled specimens do not show any variation in strength within the test-temperature range. This leads to the conclusion that once cycled, the number of cycles has negligible effect on the flexural strength. Moreover, the load-carrying capability up to 1371 °C shows the thermal stability of SiC-coated C/C up to this temperature in air.

The load–deflection behaviour of virgin material at various temperatures is shown in Fig. 4. Brittle behaviour of the material at all temperatures is noticeable from the extreme linear curves. Strain to failure is observed to decrease with the rise in temperatures. Because the failure was always on the tensile side with the virgin materials, increase in slopes indicates the increase in fibre stiffening with the rise in temperatures. The same trend of fibre stiffening has been observed with mission-cycled materials. This can be explained from the fact that the thermal expansion of the yarn is negative along the longitudinal axis and positive in the transverse direction [18]. The negative thermal expansion makes the fibre bundle stiffer at higher temperatures, causing the fibre-deflection to decrease, without decreasing its load-carrying

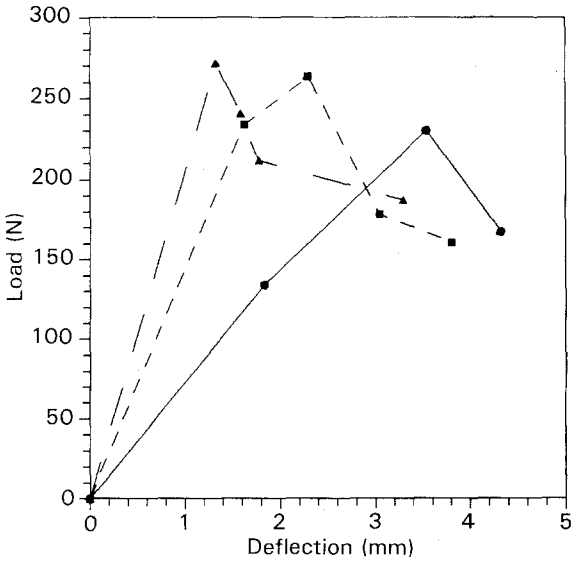

Figure 4 Load–deflection behaviour of virgin specimens at various temperatures: (●) RT, (■) 649 °C, (▲) 1371 °C.

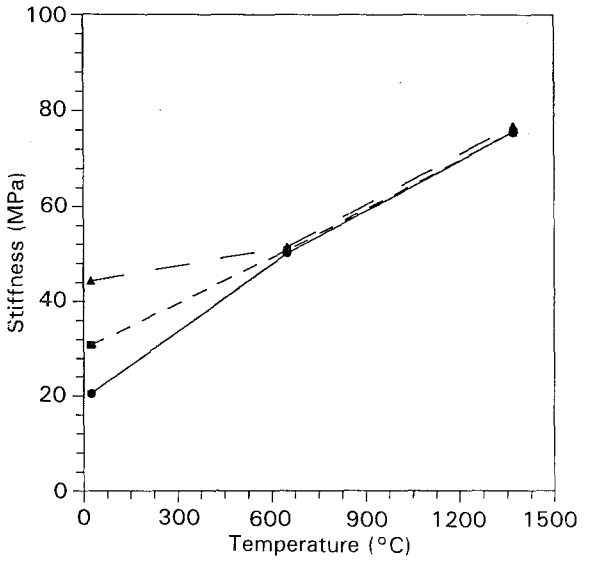

Figure 5 Flexural stiffness variation with temperatures. (●) Virgin, (■) 5 and (▲) 10 mission specimens.

capacity. This leads to the increase in stiffness at elevated temperatures, as shown in Fig. 5. The distribution of stiffness with temperatures for all types of material is shown in this figure. Load–deflection behaviour of virgin and mission-cycled materials at 649 °C is shown in Fig. 6. It is observed that the mission-cycled materials tend to fail in a ductile manner at that temperature. The ductile failure of mission cycled two-dimensional C/C is contradictory to the catastrophic failure of three-dimensional C/C during compression as reported by Robinson and Francis [17].

Weibull analyses of flexural strength and stiffness for 5 mission-cycled specimens at various temperatures are shown in Figs 7 and 8, respectively. This analysis has been performed to determine the scattering in the flexural data. In Fig. 7, the Weibull distribution, β, lies between 11.82 and 18.47. The Weibull distribution, β, is the slope of straight line and is termed as shape factors (SF) in the figures. These values of β suggest moderate scattering of flexural data, both at room and elevated temperatures. The Weibull distribution for flexural stiffness varies between 14.69 and 19.56. Weibull distribution in the similar range was also observed with whisker-reinforced ceramic matrix composites in a previous study [19]. Figs 7 and 8 also show the characteristic lives (CL) of the material at various temperatures. These characteristic lives are taken at 63.2% of the stress distribution, and are independent of the Weibull modulus. The CL also suggest the increase in flexural strength and stiffness with increasing temperature. It should be mentioned here that more meaningful Weibull analysis could be obtained using more sample data points. However, the high cost of C/C specimens limited the number of specimens to only four at each stress level during the current research.

The inherent problem of having porous matrix in C/C composites due to the fabrication or manufacturing process is shown in Fig. 9. The clearly visible pores in the matrix region suggests that the improvement in manufacturing processes is still needed. The

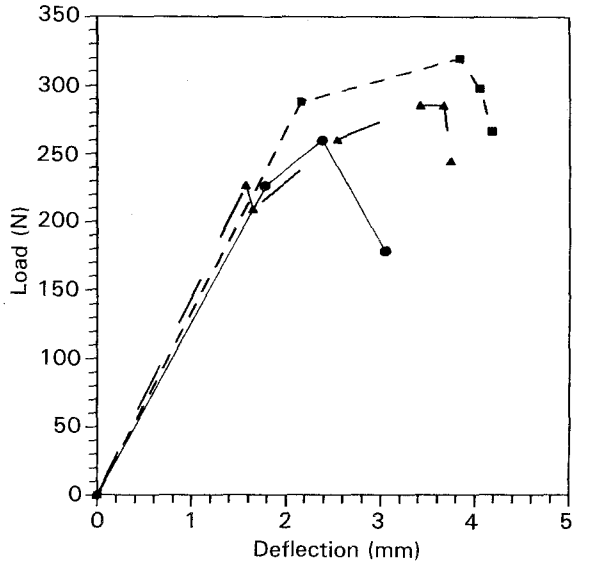

Figure 6 Comparison of load–deflection behaviour for virgin, 5 and 10 mission-cycled materials at 649 °C. For key, see Fig. 5.

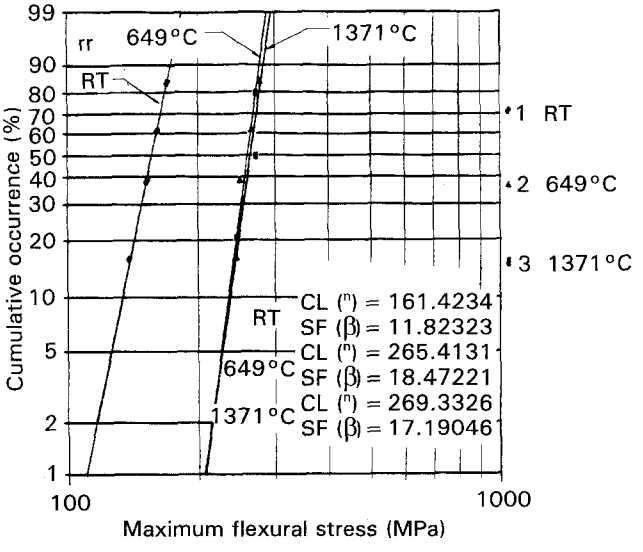

Figure 7 Weibull analysis of flexural strengths at various temperatures for 5 mission-cycled specimens.

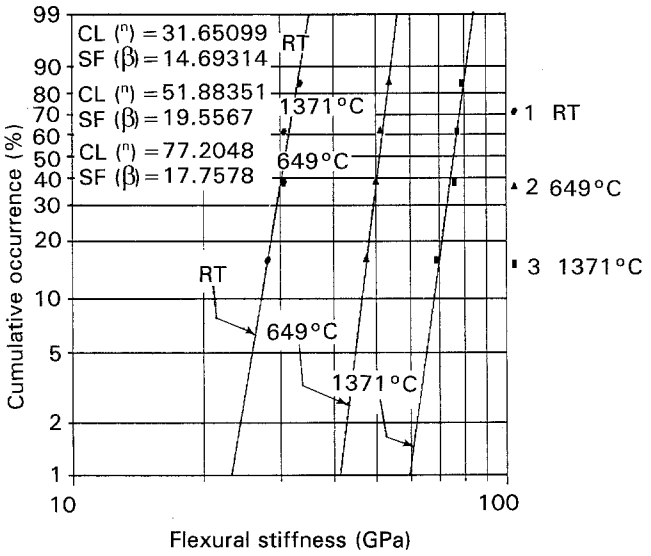

Figure 8 Weibull analysis of flexural stiffness at various temperatures for 5 mission-cycled specimens.

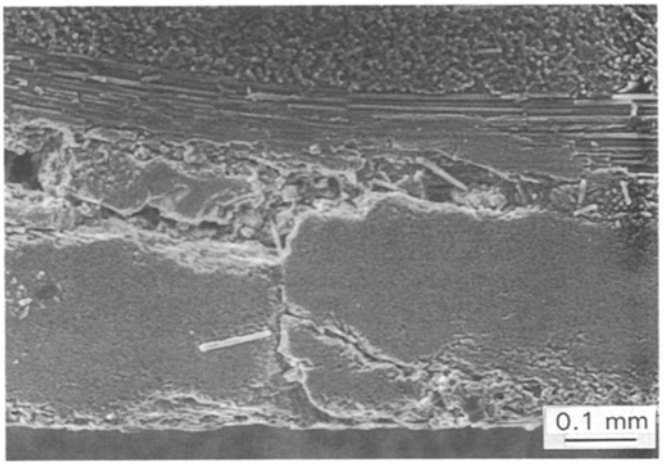

Figure 10 Typical crack propagation during high-temperature flexural test.

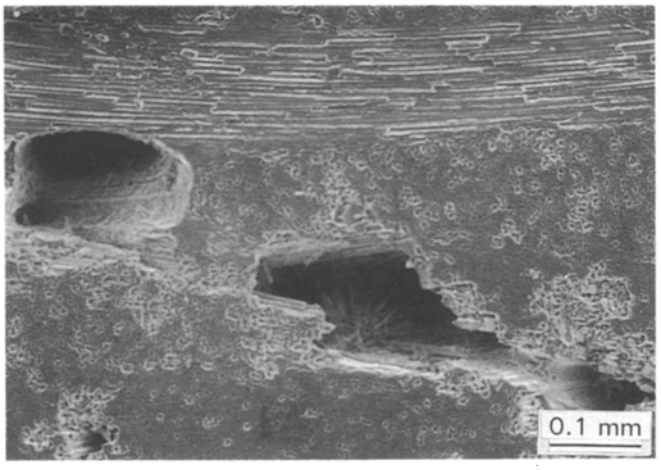

Figure 9 Porous matrix structure.

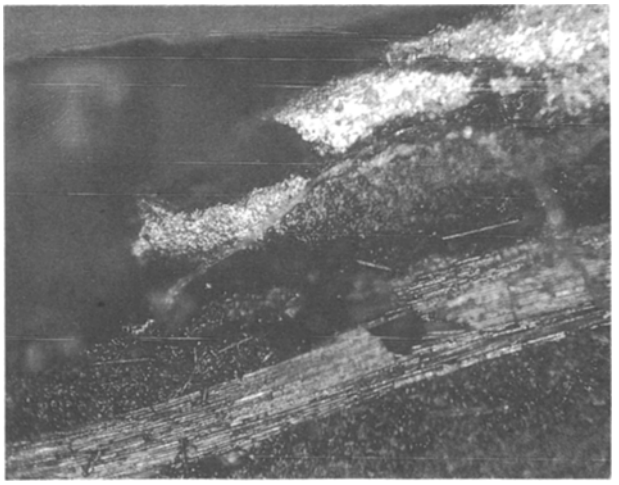

Figure 11 Complete fibre bundle failure at 649 °C (tensile side, 10 mission).

scattering of the data which has been found in the Weibull analysis, is mainly due to these types of defect or discontinuity in the matrix structure. As mentioned before, the major damage was found to be only on the tensile side of the specimen. In all cases, except for mission-cycled at RT, the crack, as shown in Fig. 10, has initiated from the outermost layers, propagated through the coating in the thickness direction, been impeded at the fibre bundle and then deflected towards the supporting ends. This crack propagation towards the ends has been observed to be along the fibre bundle, near the matrix fibre interface, but within the matrix region. From this observation, it can be concluded that the bonding between the fibre bundles and the matrix region is stronger than the matrix shear strength. Both at room and elevated temperatures, the crack stops well before reaching the support point suggesting that the damaged zone is centred in the vicinity of the loading plane. The complete failure of a fibre bundle at elevated temperature is shown in Fig. 11. The fibre bundle in the picture is in the longitudinal cross-section, and on the tensile side of the specimen. Such complete failure of the fibre bundle has not been observed in any other specimen except those at high temperature. Fibres in a transverse cross-section of the same specimen is shown in Fig. 12. A parallel finite element study [20] of this laminate has shown positive strains and tensile stresses in the transverse direction. The numerous micro failures in the filament (fibre), as shown in Fig. 12, are believed to be due to this positive transverse strain. The fibre bundle did not fail completely because of the lesser strain in that direction. Compressive failure of mission-cycled specimens at room temperature is shown in Fig. 13. Few fibre breakages can be seen; however, the failure took place mainly because of the matrix separation and this type of failure was only observed in the mission-cycled materials at RT. The extent of damage in the laminate during the room-temperature test is shown in Fig. 14. This figure shows the ultrasonic C-scan of the failed specimen. The damaged zone, as stated earlier, is within the vicinity of the loading plane, and is nearly symmetrical about that plane. This also confirms the previous FEM study [20]. It is interesting to note that the areas near the support ends of the laminate show no indication of damage during flexure tests. This is

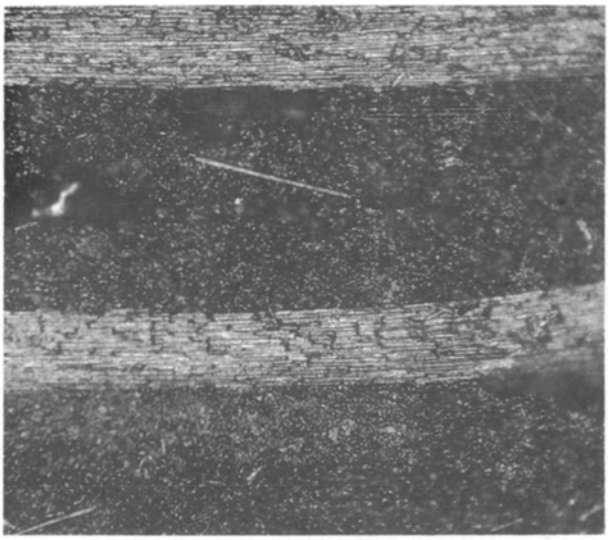

Figure 12 Filament failures in the fibre bundle (10 mission, 649 °C).

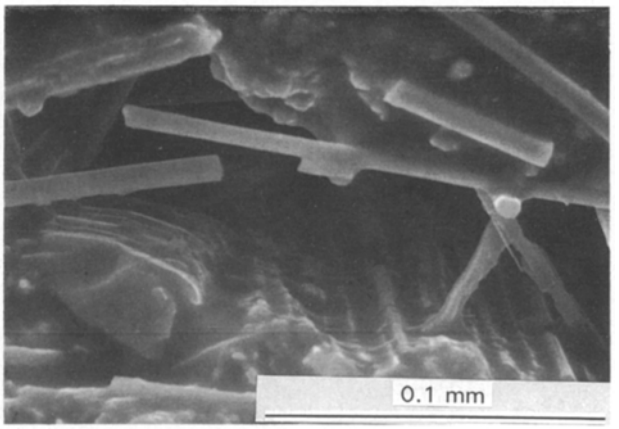

Figure 13 Failure on the compression side (5 mission, RT).

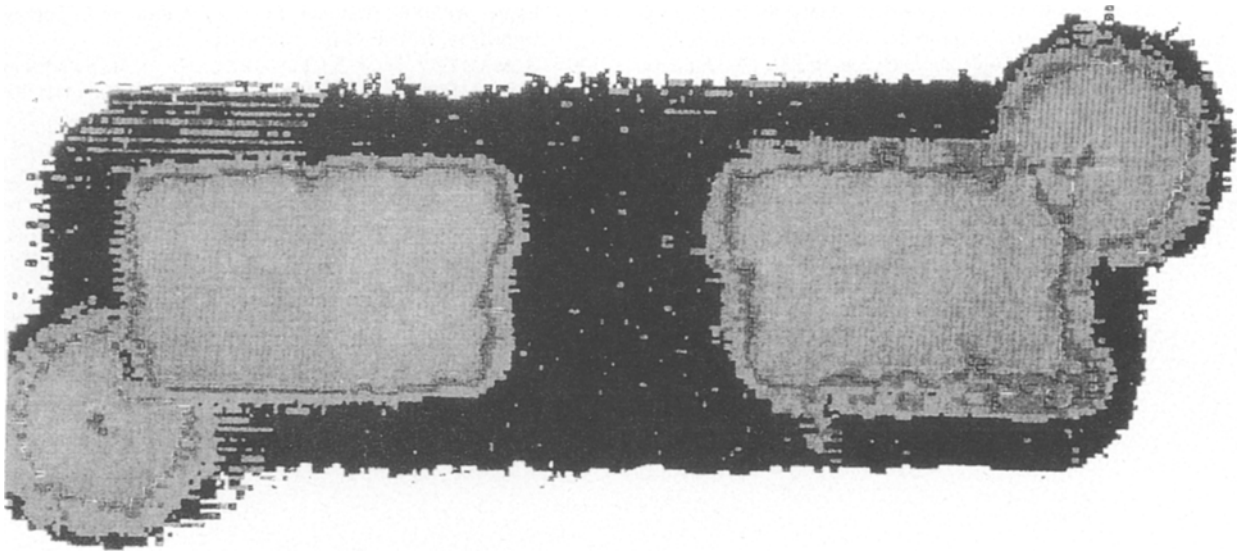

Figure 14 Ultrasonic C-scan of failed specimen (virgin, 1371 °C).

contrary to what has been reported by Copp *et al.* [8]. It is believed that the higher span to depth ratio ($L/d = 37.5$) used in the current research is the reason for localizing the damage only near the loading plane.

4. Conclusions

1. Virgin as well as mission-cycled carbon/carbon appears to be a stable system up to 1371 °C (2500 °F) under flexural load.
2. Flexural strength and stiffness increase for both virgin and mission-cycled specimens as temperature increases from room temperature to 1371 °C (2500 °F).
3. Once mission-cycled, the number of mission cycles has negligible effects on the flexural strength of C/C.
4. At elevated temperature, the failure mode is always tensile, while at room temperature, it is compressive for mission-cycled and tensile for virgin specimens.
5. The Weibull analysis shows moderate scatter in flexural strength as well as in stiffness, and predicts characteristic lives close to the average values. The Weibull distribution of C/C was also found to be similar to those of whisker-reinforced ceramics.
6. The extent of the damaged zone in the laminate is found to be within the vicinity of the loading plane and is uniformly distributed throughout the width of the specimen.

Acknowledgement

The authors acknowledge with appreciation the support for this work from the NASP/JPO through contract no. NASI-19157.

References

1. J. E. SHEEHAN, in "Engineered Materials Handbook, 1, Composites" edited by H. F. Brinson (ASM International, Metals Park, OH, 1988).
2. A. LEVINE and W. CHARD, paper presented at the 12th Biennial Conference on Carbon, American Carbon Society, St. Marys, PA, July 1975.

3. C. R. ROWE and D. L. LOWE, "High Temperature Properties of Carbon Fibres", 13th Biennial Conference on Carbon, Extended Abstract, St. Marys, PA, July 1977 p. 70.
4. "Strategic Materials: Technologies to Reduce US Import Vulnerability", Office of Technology Assessment, Congress of the United States, Washington, D.C., OTA-ITE-248, May 1985 (Congress of the United States Washington DC.
5. H. PERECHANIAN, D. JOHNSON and J. TRACY, in "Metal Matrix, Carbon and Ceramic Matrix Composites–1987", Proceedings of a Joint NASP/DoD Conference, Cocoa Beach, FL, January 1986 (American Ceramic Society, Westerville, OH).
6. D. McKEE, in "Fundamentals of Carbon-Carbon Conference", NIST, sponsored by AFOSR, Gaithersburg, Maryland, December 1990.
7. H. MARSH and J. SMITH, in "Analytical Methods for Coal and Coal Products", Vol. II, edited by Clarence Karr Jr, (Academic Press, New York, 1978).
8. P. D. COPP, J. C. DENDIS and S. MALL, *J. Compos. Mater.* **25** (1991) 593–8.
9. P. THROWER, in "Fundamentals of Carbon-Carbon Conference", NIST, Sponsored by AFOSR, Gaithersburg, Maryland, December 1990.
10. J. T. HARDING, R. A. HOLZL, R. B. KAPLAN, H. O. PIERSON and R. H. TUFFIANS, in "Metal Matrix, Carbon and Ceramic Matrix Composites–1987", Proceedings of a Joint NASP/DoD Conference, Cocoa Beach, FL, January, 1986 (American Ceramic Society, Westerville, OH).
11. X. XIAOCHENG and S. WENZHI, in "Proceedings of the 8th International Conference on Composite Materials (ICCM/8)", Honolulu, 15–19, July 1991 (Society for the Advancement of Materials and Process Engineering, Covina, CA), pp. 39-F-1–39-F-10.
12. B. MOUHAMATH, A. R. BUNSELL and T. MASSARD, *ibid.*, pp. 39-A-1–39-A-11.
13. D. J. HAGEMAIR and R. H. FASSBENDER, *Mater. Eval.* **43** (1985) 556.
14. W. WEIBULL, *Ing. Vetenskaps Akad, Handl.* **151** (1939) 5.
15. J. M. WHITNEY, I. M. DANIEL and B. PIPES, "Experimental Mechanics of Fibre Reinforced Composite Materials", Society of Experimental Stress Analysis, Monograph 4 (The Society for Experimental Stress Analysis, Brookfield Center, Connecticut).
16. R. A. LOWDEN and K. L. MORE, *Mater. Res. Soc. Symp. Proc.* **170** (1990).
17. C. T. ROBINSON and P. H. FRANCIS, in "Fatigue of Fibrous Composite Materials", ASTM STP 723 (American Society for Testing and Materials, Philadelphia, PA, 1981) pp. 85–100.
18. R. J. KERANS and K. T. FABER, in "Metal Matrix, Carbon and Ceramic Matrix Composites–1987", Proceedings of a Joint NASP/DoD Conference, Cocoa Beach, FL. January 1986 (American Ceramic Society, Westerville, OH).
19. S. JEELANI, H. MAHFUZ, D. P. ZADOO and F. WILKS, Technical Report Submitted to US Navy, ONR and US Air Force, AFOSR, Material Research Laboratory, Tuskegee University, July, 1991 (Unpublished).
20. H. MAHFUZ, D. W. XUE, S. JEELANI, D. M. BAKER and S. A. JOHNSON, *Devel. Theor. Appl. Mech.* **16** (1992) III. I. 62.

Received 21 July 1992
and accepted 4 January 1993